Available online at www.sciencedirect.com
ScienceDirect
Journal of Sound and Vibration 324 (2009) 1124–1140
JOURNAL OF SOUND AND VIBRATION
www.elsevier.com/locate/jsvi

Sound quality estimation for nonstationary vehicle noises based on discrete wavelet transform

Y.S. Wang[a,b,*]

[a]College of Automotive Engineering, Shanghai University of Engineering Science, Shanghai 201620, China
[b]School of Automobile and Traffic Engineering, Liaoning University of Technology, Jinzhou 121001, China

Received 23 September 2008; received in revised form 17 January 2009; accepted 21 February 2009
Handling Editor: L.G. Tham
Available online 25 March 2009

Abstract

A new method based on the discrete wavelet transform (DWT) for sound quality estimation (SQE) of nonstationary vehicle noises is presented in this paper. Sample interior and exterior vehicle noises are first measured and denoised using the wavelet threshold method to initially lower the noise level with negligible signal distortion. A multirate filter bank combined by a set of low-pass and band-pass filters and a DWT-based filter bank are then developed for sound octave-band analysis (OBA). To build the DWT octave-band filters, the Mallat pyramidal algorithm is introduced, and five types of wavelet function with different filter lengths are investigated and compared. Finally, the Daubechies wavelet with a filter order of 35 is determined and applied to estimate sound pressure levels (SPLs) of both the interior and exterior vehicle noises. Verification results show that the newly proposed multirate-filter-based method (MF-OBA) and DWT-based method (DWT-OBA) are accurate and effective for SQE of nonstationary vehicle noises. Due to outstanding time-frequency characteristics of the wavelet analysis, the DWT-OBA can be suggested to deal with not only SQE of nonstationary vehicle noises, but also any other sound-related signal processing in engineering.

1. Introduction

Reduction of the ever-increasing noise levels in the environment may improve our quality of life. Vehicle noises, which constitute about 40% of city environmental noise, have been considered in the past few decades, and vehicle noise control has accordingly become a very active research area. A large research effort related to SQE of vehicle noises has recently been conducted [1–3]. It has been found that the characteristics of a sound as it is perceived are not exactly the same as the characteristics of the sound being emitted. Thus, many psychoacoustic indices, such as A-weighted sound pressure level (SPL), loudness, sharpness, roughness, pleasantness, etc., have been applied to evaluate vehicle noises [4–6]. An intelligent SQE technique so-called wavelet pre-proceeding neural network (WT-NN) model for sound loudness and sharpness prediction of vehicle interior noises was developed in Ref. [6]. The International Standardization Organization (ISO) had

*Corresponding author at: School of Automobile and Traffic Engineering, Liaoning University of Technology, No. 169, Shiying Jie, Guta District, Jinzhou 121001, China. Tel.: +86 416 4199732; fax: +86 416 4199267.
E-mail address: jzwbt@163.com

0022-460X/$ - see front matter © 2009 Elsevier Ltd. All rights reserved.
doi:10.1016/j.jsv.2009.02.034

generalized SQE methods into two classes. The first is the octave-band analysis (OBA) for linear and/or weighted SPLs. The second is referring to more appropriate values based on the human sensation of loudness. Typically, the standard ISO 532 and its improved versions BS 5727 and EN 61260, which provide a graphic method for loudness calculation by means of third-octave bands, have been proven very useful for SQE designing in the automotive engineering in the areas of engine noises, vehicle interior noises, and door-slam quality [7–10]. In these works, however, only the non-unique sound signals can be considered, because the stationary frequency-based techniques were performed in the SQE procedures. In cases of the nonstationary vehicle noises, these frequency-based techniques are not appropriate for direct SQE; therefore, it is both necessary and useful to find new methods for accurate evaluation of nonstationary sound qualities.

In SQE engineering, digital signal processing (DSP) techniques need to be carefully selected according to characteristics of the sound signals of interest. For nonstationary signal processing, some time-frequency techniques in common use, which are suitable for extracting transient signal features, have been frequently mentioned in the literature [11–14]. Short-time Fourier transform (STFT) uses a standard Fourier transform over several types of windows. Wavelet-based techniques can apply a mother wavelet function with either discrete or continuous scales to surmount the fixed time-frequency resolution issue inherent in STFT. In applications, the discrete versions, such as the discrete wavelet transform (DWT) and wavelet packet analysis (WPA), are usually used for reducing the number of calculations to be done, thereby saving computer running time. An efficient way to implement the DWT was developed by Mallat in 1989 [15]. The Mallat algorithm, which is in fact a canonical scheme known in signal processing community as a two-channel sub-band coder, yields a fast wavelet transform (FWT) and make the DWT more powerful for solving practical problems [16]. As such, of the three wavelet techniques, the DWT is suggested as a useful tool in engineering for nonstationary vibration and sound signal analysis [17–19]. In recent years, the DWT-based techniques and their improved versions, such as the constrained adaptive lifting wavelet algorithm, wavelet denoising methods, and the integrated wavelet identification, etc., have been widely used for the machinery failure diagnosis, condition monitoring, uncertain modal analysis, and also the contaminated signal denoising in engineering [20–22]. Ambiguity functions (AF) and Wigner–Ville distributions (WVD) have better resolution than STFT, but suffer from cross-term interference and produce results with coarser granularity than wavelet techniques do [6,11]. Almost all vehicle noises in actual working cases, such as those generated in acceleration and deceleration processes, are nonstationary. Based on the above findings, the STFT, DWT, and WPA may be regarded as the candidate techniques for real-time analysis of nonstationary sound signals. The purpose of this paper is to develop a new OBA method for nonstationary vehicle noises. Considering the inherent frequency partitions of the OBA in ISO standards, therefore, the DWT techniques are adopted in this present work.

From the above discussions, we concluded that the in-situ frequency-based OBA approaches, as the basic method for SQE, cannot directly be used to process nonstationary sound signals. Based on a measured interior vehicle noise, a new OBA technique based on the wavelet transform, so-called DWT-OBA, is developed in this paper. The DWT-OBA method may directly be used to estimate not only nonstationary, but also stationary and even transient sound qualities in vehicle engineering. In view of the application, it may also be extended to more general cases for sound quality evaluations of any other sound signals in engineering.

2. Theory background

2.1. Digital filtering techniques

The technique of infinite impulse response (IIR) filter is adopted to design a frequency-based octave filter bank in this paper. An one-dimensional digital IIR filter can be represented by its impulse response sequence, $h(k)$ ($k = 0,1,2,\ldots$). The input signal $x(t)$ and output signal $y(t)$ to the digital IIR filter, which are related by the convolution sum, can be given as:

$$y(t) = \sum_{k=0}^{\infty} h(k)x(t-k) = \sum_{k=0}^{N} b_k x(t-k) - \sum_{k=1}^{M} a_k y(t-k) \tag{1}$$

where the a_k and b_k are the coefficients of the filter, and $t = 1,2,3,\ldots,N$. Alternatively, the transfer function of the IIR filter in frequency domain can be represented in Z-transform as

$$H(z) = \frac{\sum_{k=0}^{N} b_k z^{-k}}{1 + \sum_{k=1}^{M} a_k z^{-k}} \tag{2}$$

where, $H(z)$ is the complex frequency response of the filter, $z = e^{jw}$ is the operator of Z-transform.

2.2. Discrete wavelet transform

Wavelet transform (WT) is widely used in various subfields of mathematics, science, and engineering. WT is the process of decomposing or reconstructing a signal using wavelets, a family of orthogonal functions of type,

$$\Psi_{a,b}(t) = |a|^{-1/2}\psi[(t-b)/a] \quad a, b \in, \;\; R \;\; a \neq 0 \tag{3}$$

generated from a 'mother' wavelet function $\psi(t)$ by dilation and translation operations, which are governed by the scale factor a and shift factor b. The continuous wavelet transform (CWT) of a signal $f(t) \in L^2(R)$ has been defined in Ref. [14].

The DWT involves choosing scales and positions based on powers of two, so called dyadic scales and positions. The mother wavelet is rescaled or dilated by powers of two and translated by integers. Setting the scale and shift factors to $a = a_0^{-j}$, $b = a_0^{-j} k b_0$ ($j, k \in Z$, $a_0 > 1$, $b_0 > 0$), the continuous wavelet function becomes $\psi_{j,k}(t) = a_0^{j/2}\psi(a_0^j t - nb_0)$. If $a_0 = 2$, $b_0 = 1$, and the DWT and its reconstructed version may be written in a dyadic discrete form,

$$W_f(a,b) = W_f(2^{-j}, 2^{-j}k) = 2^j \int_{-\infty}^{+\infty} \psi(2^j t - k) f(t)\, \mathrm{d}t \tag{4}$$

$$f(t) = \sum_j \sum_k W_f(2^{-j}, 2^{-j}k)\psi(2^j t - k) \tag{5}$$

2.3. Mallat pyramidal algorithm

Based on a concept of multi-resolution analysis, the Mallat pyramidal algorithm is in fact a classical scheme known as a two-channel sub-band filter. Using this method, a signal $f(t) \in L^2(R)$ may be approached by a set of approximations with different resolutions.

Let $A_L[\cdot]$ and $D_L[\cdot]$ be a pair of operators for L-level signal decomposition (or reconstruction). At jth level, $A_j[f(t)]$ and $D_j[f(t)]$ represent the approximation and detail of signal $f(t)$, respectively. The decomposition signals may be characterized by inner multiplying the scale function φ and wavelet function ψ of a selected WT with the signal $f(t)$. Therefore, the decomposition equations of the Mallat algorithm can be expressed as follows:

$$A_0[f(t)] = f(t) \tag{6}$$

$$A_j[f(t)] = \langle f(t), \varphi_{j,t} \rangle = \sum_k H_{k-2t} * A_{j-1}[f(t)] \tag{7}$$

$$D_j[f(t)] = \langle f(t), \psi_{j,t} \rangle = \sum_k G_{k-2t} * A_{j-1}[f(t)] \tag{8}$$

where $t = 1,2,3,\ldots,N$ ($t \in Z$), $j = 1,2,3,\ldots,J$ ($j \in Z$), and $J = \log_2 N$. H and G are a pair of quadrature mirror filters for decomposition. H is a low-pass filter and G is a high-pass filter. Their impulse responses $\{H_n\}_{n \in z}$ and $\{G_n\}_{n \in z}$ satisfy the equations $\sum H_{n-2k} H_{n-2m} = \delta_{k,m}$, $\sum H_n = \sqrt{2}$, and $G_n = (-1)^n H_{1-n}$, respectively. The $A_j[f(t)]$ and $D_j[f(t)]$ may be obtained by feeding $A_{j-1}f$ to the filters H and G, respectively, and desampling the output signals. The DWT calculation procedure based on the Mallat algorithm is shown in Fig. 1, where ↓2: keeping one sample out of two, ↑2: putting one zero between two samples, $\boxed{G}$, $\boxed{H}$, $\boxed{g}$, and $\boxed{h}$: convoluting with G, H, g, and h, respectively.

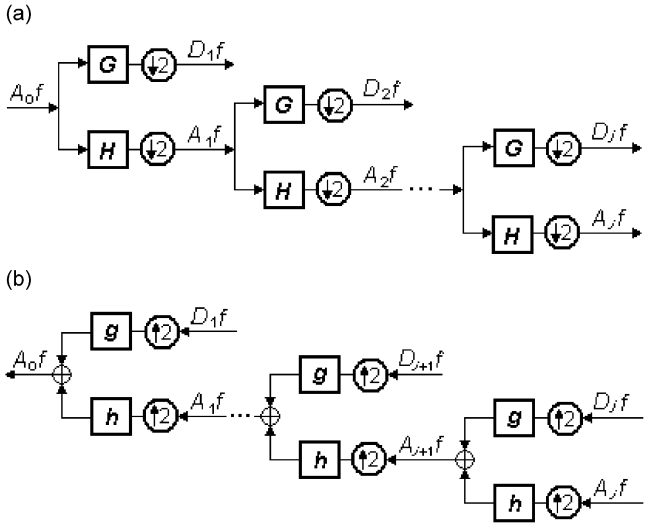

Fig. 1. DWT multi-resolution analysis using Mallat pyramidal algorithm: (a) decomposition and (b) reconstruction.

For the wavelet reconstruction, inversely, one may up-sample (insert zeros) the $A_{j+1}[f(t)]$ and $D_{j+1}[f(t)]$ first, and then pass them through the mirror filters h and g for constructing $A_j[f(t)]$. The reconstruction equation of the Mallat algorithm is,

$$A_j[f(t)] = \langle f(t), \varphi_{j,t} \rangle = \sum_k h_{t-2k} * A_{j+1}[f(t)] + \sum_k g_{t-2k} * D_{j+1}[f(t)] \tag{9}$$

where $t = 1,2,3,\ldots,N$ ($t \in Z$), $j = 1,2,3,\ldots,J$ ($j \in Z$), and $J = \log_2 N$. h and g are a pair of quadrature mirror filters for reconstruction. h is a low-pass filter and g is a high-pass filter. Their impulse responses $\{h_n^*\}_{n \in z}$ and $\{g_n^*\}_{n \in z}$ can be directly calculated by the impulse responses of H and G as: $h_n^* = H_{-n}$ and $g_n^* = G_{-n}$.

3. Acquisition and pre-processing of vehicle noises

In this paper, the interior and exterior vehicle noises are prepared by using the binaural recording technique [5]. In the measurements, a sample vehicle is accelerated up to a running speed 50 km/h [23]. The following parameters for data acquisition are used: signal length, five seconds, sampling rate, 50 kHz. The measured sound signals need to be denoised for avoiding signal distortion by certain additive noises, which maybe came from the ambient noise and/or the hardware of the measurement system. The wavelet threshold method has been proved very powerful in denoising of nonstationary signals [6]. Therefore, in this paper, a DWT denoising procedure is performed in three steps: (a) signal decomposition, (b) threshold determination, and (c) signal reconstruction. The soft threshold signal is $sign(x)$ $(|x|-t)$ if $|x| > t$, and otherwise is 0, where t denotes the threshold. The selected parameters are: Daubechies wavelet '*db*3', seven levels, soft universal threshold equals to the root square of $2\log(length(f))$. The denoised interior noise and its spectrum are shown in Fig. 2. Here note that several new nonlinear filters for removing noise and outliers from the nonstationary, or even transient signals, such as the weighted recursive median filter (WRM), radial basis function (RBF) neural networks, adaptive myriad filter (AMF), and the subfilter weighted FIR median hybrid (SWFMH) filter, have been developed and applied [20,24–26]. The validity investigation of these filters in vehicle sound denoising will be another discussion topic in our future work.

During the data acquisitions, meanwhile, the sound level meter NL-27 is used for measuring the equivalent SPL values of both the interior and exterior noises. The averaging time intervals were set to the same as the length of signals, 5 s. The measured SPLs can be used to validate the newly developed methods and will be mentioned in the following text.

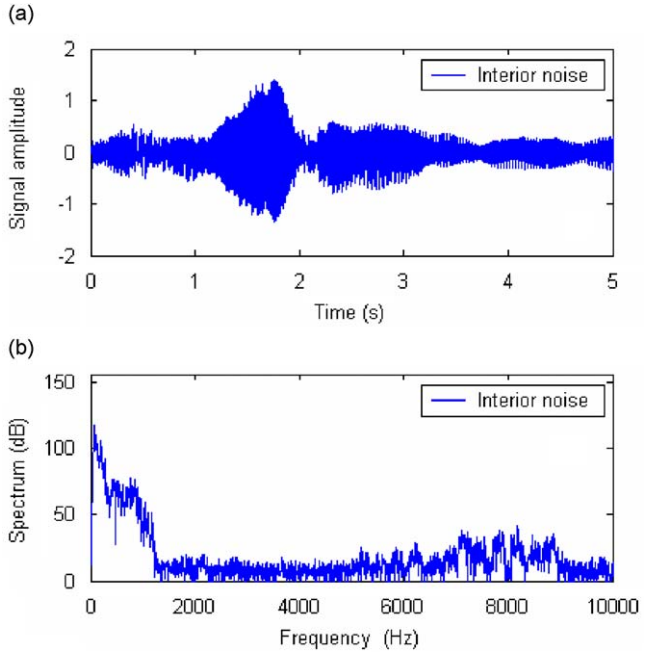

Fig. 2. A measured and denoised vehicle interior noise during acceleration: (a) noise signal and (b) signal spectrum.

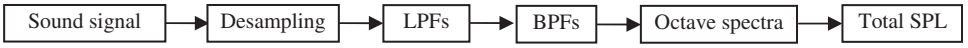

Fig. 3. Filter bank implement for octave-band analysis of a sound signal.

4. Filter bank design and implement for OBA

To develop the DWT-OBA approach, as a reference, a frequency-based, multirate, octave filter band is designed for sound OBA in the Matlab Toolbox. This filter bank consists of a set of low-pass filters (LPFs) and band-pass filters (BPFs). The former is for eliminating the aliasing in the desampled signals, and the later is for extracting the octave-band SPL values, respectively. The Butterworth IIR filter is selected here. The multirate filtering OBA (hereafter called MF-OBA) of a sound may be performed following the scheme depicted in Fig. 3. The determined parameters in the designed LPFs and BPFs of the filter bank are listed in Table 1.

In the filter bank design, the digital desampling technique has to be performed, since the IIR octave filters are applicable only inside the frequency band in the range of $f_s/500$ to $f_s/4$ [27]. The original sampling rate (f_s) is 50 kHz. The sampling rates of the LBPs are specified for the corresponding octave bands of the BPFs on the purpose of signal anti-aliasing. The center frequency f_c of each octave band is defined according to the ISO standards. And the lower frequency f_l and upper frequency f_h are computed by $f_l = f_c/\sqrt{2}, f_h = \sqrt{2}f_c$. The filter coefficients a_k and b_k are determined by setting the pass-band and stop-band edge frequencies w_p and w_s to $w_s = [2f_l/\alpha, 2\alpha f_h]/f_s$, $w_p = [2f_1, 2f_2]/f_s$, and also the stop-band attenuation to 12 dB, where $\alpha = [1 + \sqrt{1 + 8\beta^2}]/4\beta$, $\beta = \pi/[2N \sin(\pi/2N)]$. N denotes the order of the filter. The filter orders of the LPFs and BPFs are fixed to 3 and 6, respectively. The transfer functions in frequency domain of the LPFs and BPFs are shown in Fig. 4.

Verification of the multirate filter bank is also conducted in this work. In Fig. 5 the self-designed band-pass filter with the center frequency $f_c = 8$ kHz is proved by using the standard IEC 1260 (class 1) [27]. Furthermore, taking the measured interior vehicle noise, the sound OBA procedure in Fig. 3 is performed, in

Table 1
The determined parameters in the designed filter bank for octave-band analysis of vehicle noises.

Octave band number	1	2	3	4	5	6	7	8	9	10
Low-pass filters (*LPFs*)										
Center frequency (Hz)	16	32	63	125	250	500	1000	2000	4000	8000
Cutoff frequency (Hz)	50	78	156	312	625	1250	2500	5000	10000	20000
Sampling rate (Hz)	781	781	781	781	1562	3125	6250	12500	25000	50000
Band-pass filters (*BPFs*)										
Center frequency (Hz)	16	32	63	125	250	500	1000	2000	4000	8000
Upper frequency (Hz)	22	44	88	177	354	707	1414	2828	5657	11314
Frequency bandwidth (Hz)	11	22	44	89	177	353	707	1414	2829	5657
Sampling rate (Hz)	98	195	390	781	1562	3125	6250	12500	25000	50000
Filter coefficients										
b_k	0.0007, 0, −0.0044, 0, 0.0111, 0, −0.0148, 0, 0.0111, 0, −0.0044, 0, 0.0007									
a_k	1, −4.73, 12.63, −23.11, 32.1, 35.0, 0.662, −21.62, 12.233, −5.417, 1.814, −0.415, 0.054									

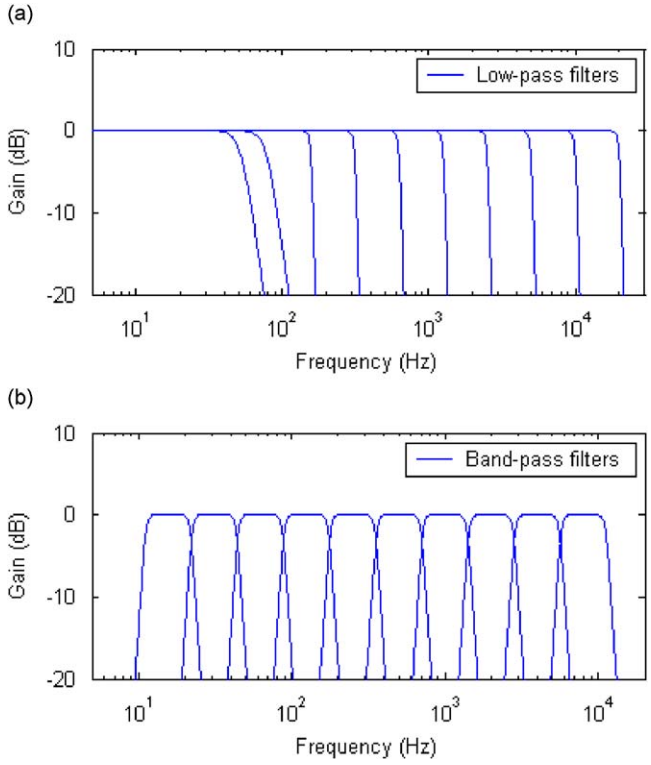

Fig. 4. Designed filter bank for octave-band analysis: (a) the anti-aliasing low-pass filters and (b) the octave band-pass filters.

which the total SPL L_T is calculated by using the following equation:

$$L_T = 10 \log\left(\sum_i 10^{L_i}\right) \tag{10}$$

where L_i is the calculated ith band SPL, i is the octave band number, $i = 1,2,\ldots,10$. Note that only 10 octaves with the center frequencies up to 8 kHz are considered here, due to the low frequency components of the vehicle noises (see Fig. 2). The calculated band SPL values are shown and compared with the measured results

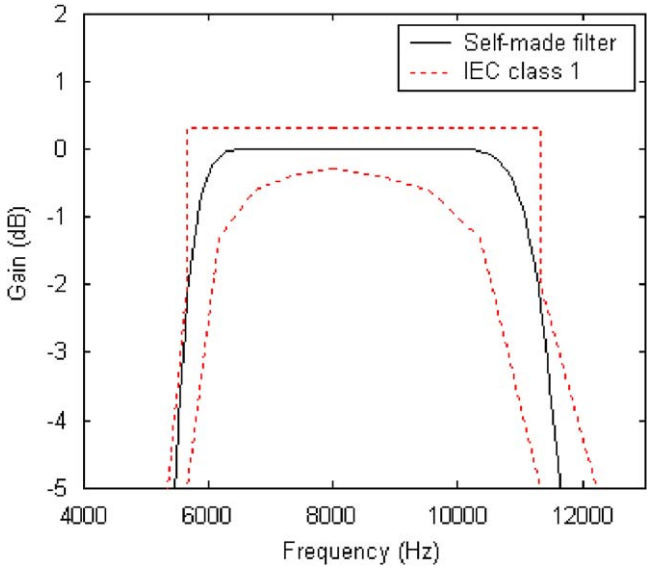

Fig. 5. Filter shape comparison between the self-designed band-pass filter and the IEC standard (class 1) ($f_c = 8$ kHz).

in Fig. 6. As seen in Fig. 6(c), the maximum error of the band linear SPL values is less than 0.3 dB. In view of the total SPL, the measured equivalent $L_T = 83.7$ dB, the calculated $L_T = 83.83$ dB. The conclusion can be drawn that the proposed MF-OBA is accurate for octave analysis of the vehicle noises and can be used as a reference in the following DWT-OBA development.

5. DWT implement for OBA

5.1. Establishment of wavelet filter bank

Before using a WT, in engineering, one has to select a wavelet function from the wavelet family for his practical purposes. The characteristics of the wavelet functions, such as orthogonality, compactly supporting and vanish moment, need to be investigated. The orthogonality is always being expected in signal processing. A compactly supported wavelet can provide a finite, more accuracy filter. The support length depends on the filter length of the wavelet. The longer the support length is, the smoother the scale function, and the less the coherence be. A high-order vanish moment can provide a rapid decay speed to the wavelet transform. To develop the DWT-OBA approach for nonstationary sound signals, in this present work, five wavelet functions in common use, such as Daubechies, Coiflets, Symlets, Discrete Meyer Wavelet, Biorthogonal and its reverse version, are considered. The names of these wavelet functions in the Matlab Toolbox and their corresponding filter lengths are listed in Table 2.

The Mallat algorithm is used for DWT calculation in this paper. For an N-level DWT, a wavelet filter bank with $N-1$ band-pass filters may be created by the Mallat algorithm, which is actually combined by N pairs of low- and high-pass filters with different sampling rates. If one properly selects the sampling rates, the wavelet band filters could be well matched to the filter bank shown in Fig. 4(b). Setting the sampling rates to 707 Hz (for high-pass filters) and to 1414 Hz (for low-pass filters), which are exactly same as the lower and upper frequencies of the 7th octave band as seen in Table 1, the frequency characteristics of the combined wavelet band filters from different wavelet functions are shown in Fig. 7. As a reference, the frequency response of the foregoing band filter with the center frequency $f_c = 1000$ Hz is drawn in the same plot. Comparison suggests that the Daubechies filter marked as '*db*35' in Fig. 7 is the closest to the octave band number seven. That means the Daubechies wavelet, which has a property of maximally flat, is the most suitable wavelet function for sound wavelet OBA. In frequency domain, the Daubechies wavelet has been defined in Ref. [28]. A larger order of the Daubechies wavelet filter p leads to a longer filter length and a better orthogonality. To determine

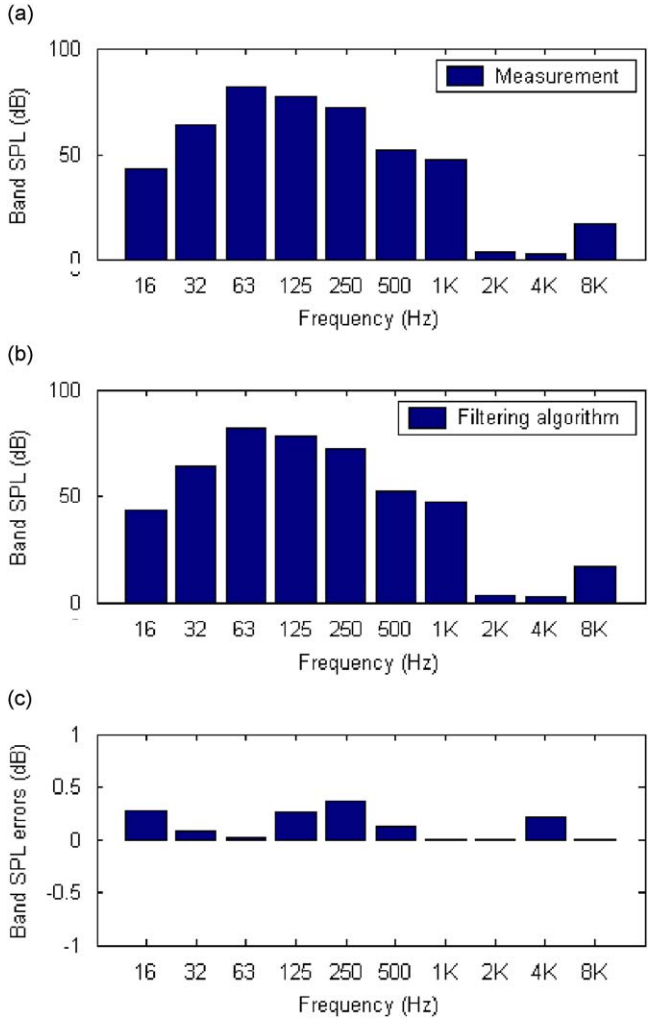

Fig. 6. Linear SPL comparison of the octave-band analysis of the interior vehicle noise: (a) the measured result, (b) SPL values calculated by the self-designed filter bank and (c) the band SPL errors.

Table 2
The candidate wavelet functions and selected parameters in DWT octave-band analysis.

Wavelet functions	Wavelet names in the Matlab Toolbox	Filter lengths	Analysis levels
Daubechies	'*db*5', '*db*10', '*db*15', '*db*P', …, '*db*45'	2P	max(band#) + 1
Coiflets	'coif1', 'coif2', 'coifP', …, 'coif5'	6P	max(band#) + 1
Symlets	'sym5', 'sym10', 'sym15', 'symP', …, 'sym45'	2P	max(band#) + 1
Discrete meyer	'dmey'	62	max(band#) + 1
Biorthogonal	'bior1.5', 'bior2.8', 'bior3.9', 'biorM.P', 'bior6.8'	max(2M,2P) + 2	max(band#) + 1
Reverse biorthogonal	'rbio1.5', 'rbio2.8', 'rbio3.9', 'rbioM.P', 'rbio6.8'	max(2M,2P) + 2	max(band#) + 1

an appropriate filter length for sound DWT-OBA, the Daubechies wavelets named '*db*5', '*db*10', '*db*15', …,'*db*45' in the Matlab Toolbox are performed and compared in Fig. 8.

As seen from Fig. 8, for the filter top part (Gain > 0.7), the longer the filter length is, the better the wavelet filter fits the referenced one, except for the '*db*45' case. The '*db*45' filter shows a fluctuating frequency feature, due to some uncertain reasons. When the filter order increasing to larger than 35, the 'skirt' part (Gain < 0.7)

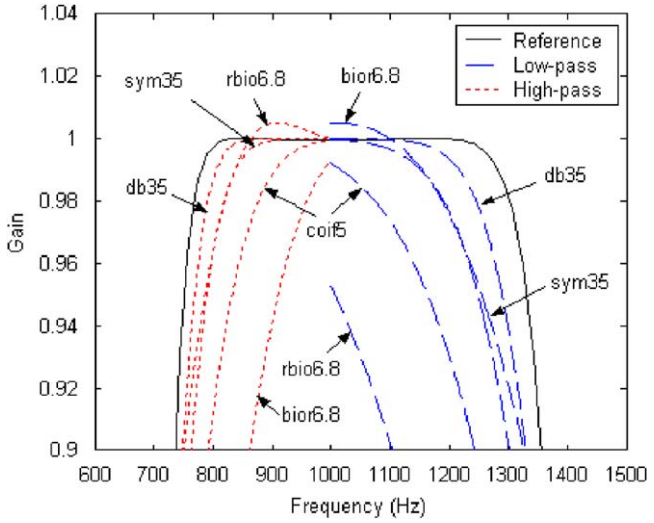

Fig. 7. Comparison of frequency characteristics of the wavelet functions in common use with different lengths of filters.

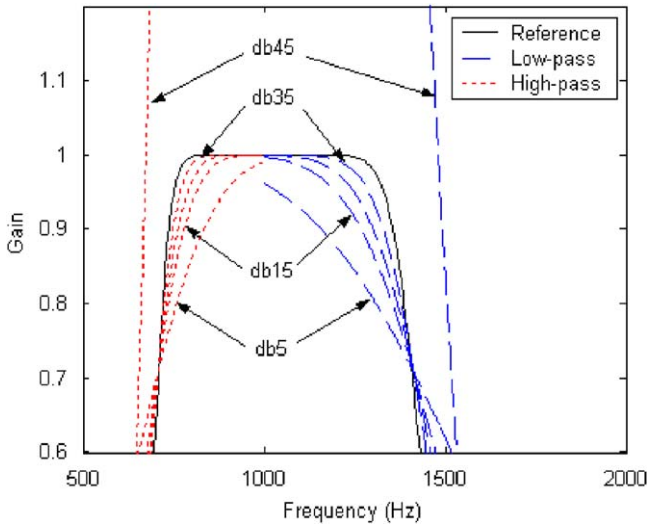

Fig. 8. Comparison of frequency characteristics of the Daubechies wavelet with different length of filters.

of the wavelet filter trends to be narrower than that of the reference filter. Considering the compromise between the properties and calculation amount of the wavelet filters, we finally select the Daubechies wavelet with filter length of 70 ($p = 35$) to build the DWT-OBA filter bank in the presented work. Setting the sampling rate of a signal to 45 256 Hz, the DWT-based filters are conducted by using the Mallat pyramidal algorithm and their frequency spectra in Decibel are shown in Fig. 9. Referring to frequency characteristics of the filter bank in Fig. 4, it is reasonable to suppose that the newly developed DWT filter bank has a good accuracy for the OBA of sound signals.

5.2. DWT-OBA and verification

Based on the measured interior vehicle noise, a DWT-OBA procedure is performed in this section. As mentioned before, the determined wavelet function is the Daubechies wavelet with filter length of 70, i.e., '*db*35'. Through the Mallat algorithm, the coefficients of the quadrature mirror filters of the wavelet function

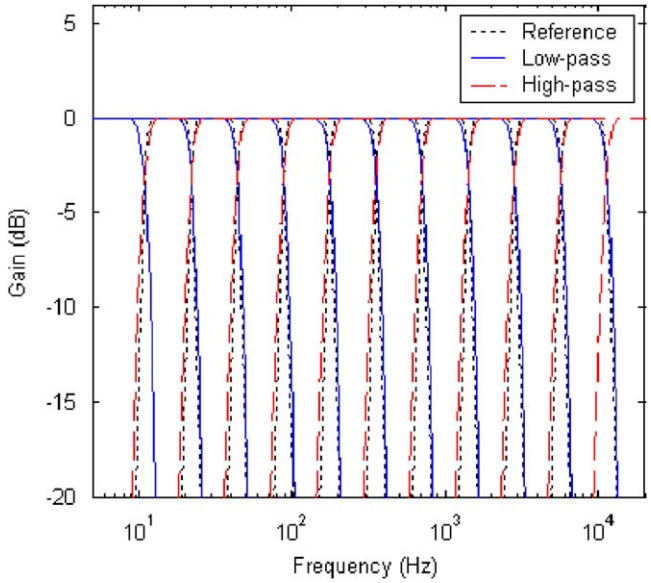

Fig. 9. Comparison of frequency characteristics between the self-designed filter bank and the Daubechies wavelet mirror filters with the length of 70.

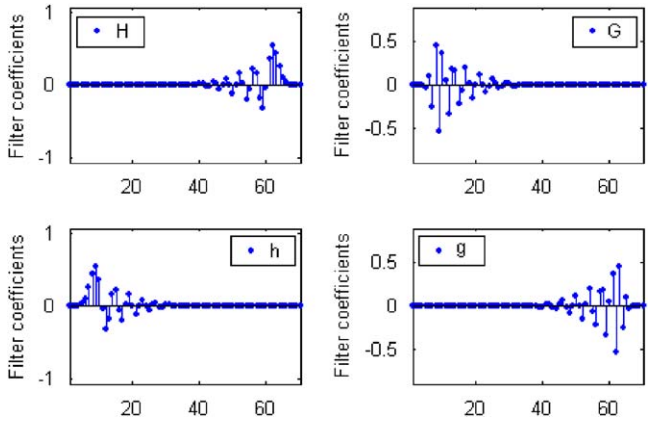

Fig. 10. Coefficients of quadrature mirror filters of the Daubechies wavelet with a filter length 70 (*db*35), where H, h, and G, g denote low-pass and high-pass filters specified for signal decomposition and reconstruction, respectively.

'*db*35' are depicted in Fig. 10, where H, h, and G, g denote the low- and high-pass filters specified for signal decomposition and reconstruction, respectively. The sound DWT-OBA of the interior noise can be performed in three steps: (a) signal resampling, (b) DWT filtering, and (c) band SPL calculation. The calculation procedure for the DWT-OBA of a sound signal is shown in Fig. 11.

To apply to DWT-based filter bank in Fig. 9, we need firstly to modify the sampling rate of the measured interior vehicle noise from 50 kHz to 45 256 Hz. This resampling procedure is realized by using the software named CoolEdit in this work.

After resampling, the interior noise signal is fed to the DWT filter bank shown in Fig. 9. This may actually be completed by applying an eleven-level DWT to the resampled interior noise. The above mentioned filters H, h, and G, g are used for signal decomposition and reconstruction, respectively.

The results of eleven-level DWT are shown in Figs. 12–14, in which the left panels are sub-band filtered (decomposed) signals and the right panels, their corresponding spectra. It can be seen that the original signal is

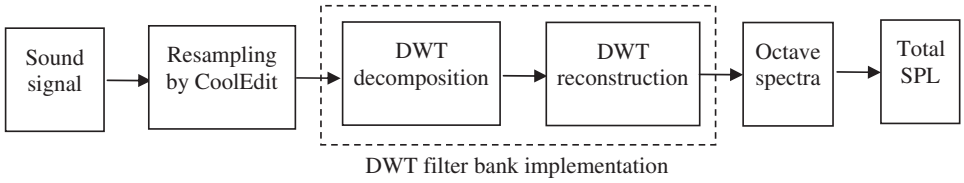

Fig. 11. The calculation flowchart for DWT octave-band analysis of a sound signal.

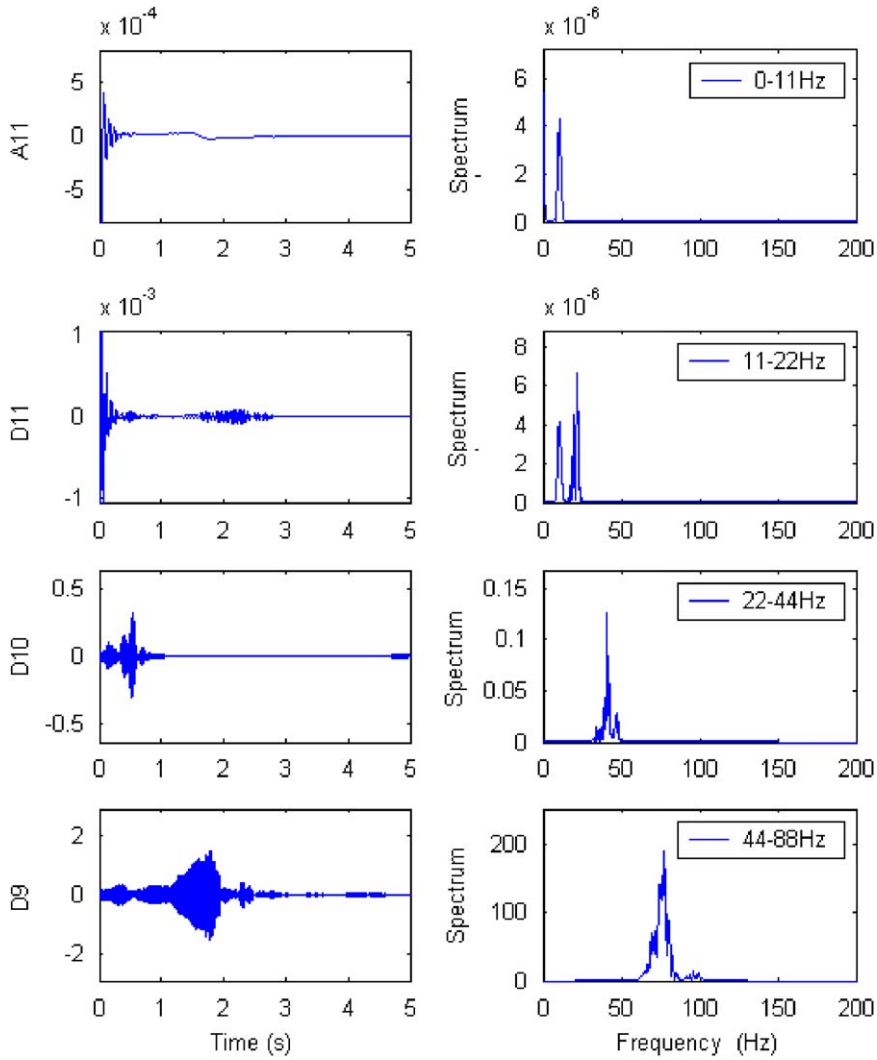

Fig. 12. Sub-band signals and their spectra after applying the *db*35 to the measured vehicle interior noise (from A11 to D9).

separated into an approximation signal (A11) and eleven detail ones (D1–D11), which lie in different frequency ranges. Due to the nonstationary characteristics of the measured interior noise, these sub-band signals with different patterns in time domain and sound energies in frequency domain may be defined as sound features of the interior noise to distinguish with other sound signals. The interior noise energy is mainly distributed in the frequency range from 22 to 707 Hz (D10–D6) in the eleven-level DWT.

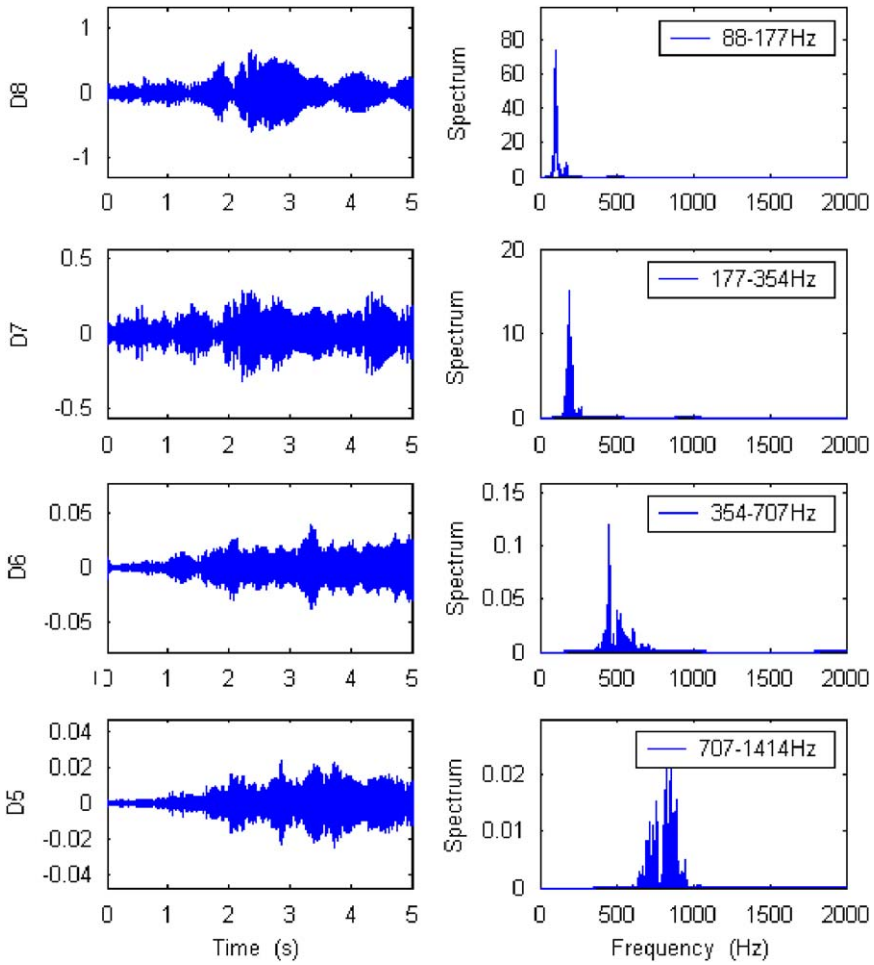

Fig. 13. Sub-band signals and their spectra after applying the *db*35 to the measured vehicle interior noise (from D8 to D5).

Finally, the octave-band SPL values can easily be calculated from the sub-band filtered signals using the definition of sound pressure level in time domain,

$$L_i = 10\log\left(\frac{1}{m_i}\sum_{j=1}^{m_i} p_{ij}^2 \Big/ p_{\text{ref}}\right) \tag{11}$$

where L_i is the ith band SPL, m_i is the total points of the ith band signal, p_{ij} is the ith band sound pressure on the jth point, and p_{ref} is the reference sound pressure, $p_{\text{ref}} = 20\text{e}{-6}$.

It can be seen from the DWT filter bank in Fig. 9, the approximation signal A11 in Fig. 12 and the detail signal D1 in Fig. 4, which are, respectively, derived from the low-pass filter with the lowest sampling rate and the high-pass filter with the highest sampling rate, should not be considered in OBA. Therefore, the linear SPL values of the sub-band signals from D11 to D2 are calculated and shown in Fig. 15. Comparing with the measured results, the errors of the band SPLs in Fig. 15(c) are within $[-0.3,\ +0.2]$ dB, which are much less than the band error scope of ± 1 dB defined in the IEC 651 standard. The total SPL are also computed by Eq. (10), it is exact same as the measured value 83.7 dB. In view of the A-weighted total SPL, the measured value is 66.1 dB(A), and the calculated value is 66.2 dB(A). To prove transient characteristic of the DWT-OBA algorithm, furthermore, the time-varying A-weighted total SPLs of the interior vehicle noise are carried out by using the newly proposed DWT-OBA and MF-OBA algorithms, respectively. According to the literature [29], the selected calculation parameters are: time frame length, 200 ms, frame amount, 25, and A-weightings,

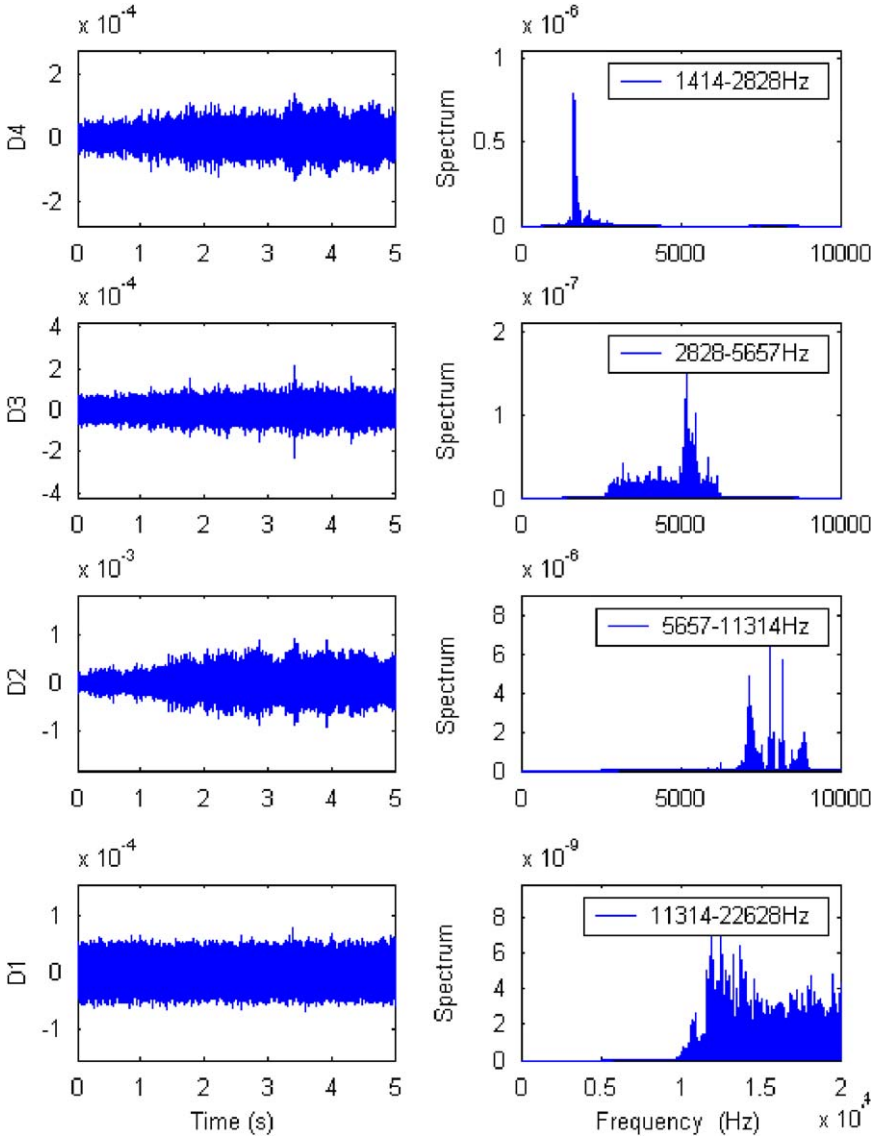

Fig. 14. Sub-band signals and their spectra after applying the *db*35 to the measured vehicle interior noise (from D4 to D1).

[−56.7 −39.4 −26.2 −16.1 −8.6 −3.2 0 1.2 1.0 −1.1] dB, for octave band number from one to 10. The results shown in Fig. 16 imply a very good transient characteristic of the DWT-OBA. Therefore, conclusion can be drawn that the DWT-based filter bank has enough accuracy for OBA and can be used to study not only stationary, but also nonstationary vehicle noises.

6. Application of the DWT-OBA

In order to examine the effectiveness the presented DWT-OBA algorithm for more practical uses, we applied it and the self-designed filtering algorithm to the measured exterior vehicle noise, respectively. The exterior noise signal shown in Fig. 17 has been pre-processed following the DWT denoising procedure in Section 3. The A-weighted band SPLs of the exterior vehicle noise calculated from the filtering and DWT algorithms, as well as the measurement results, are shown in Fig. 18. And the calculated results are summarized in Table 3. It can be seen that, for the exterior vehicle noise, the A-weighted SPLs from different

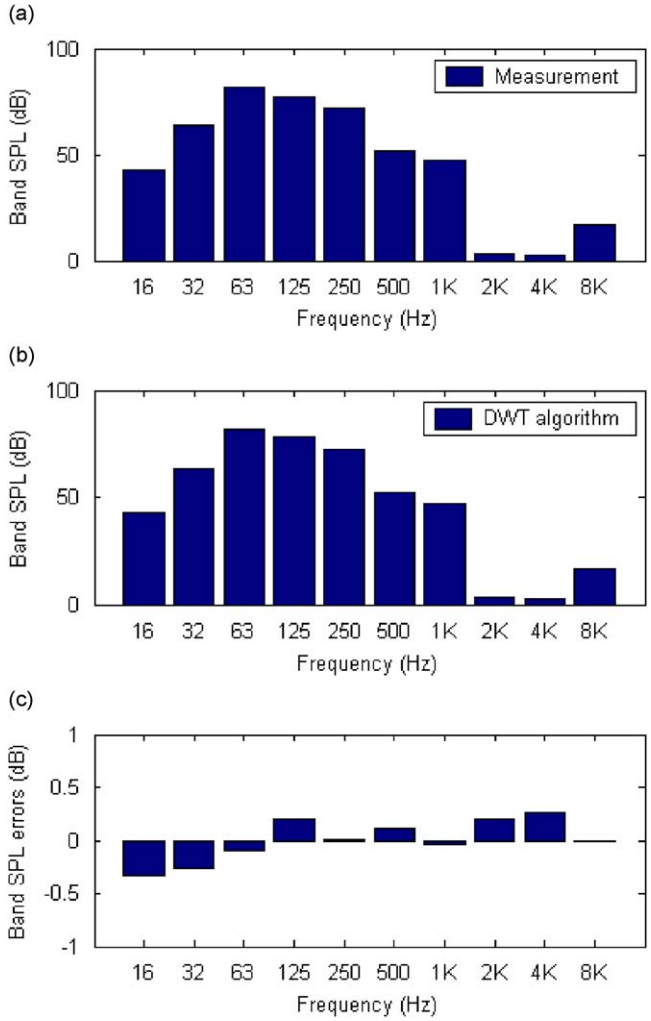

Fig. 15. Linear SPL comparison of the octave-band analysis of the interior vehicle noise: (a) the measured result, (b) SPL values calculated by the *db*35 filter bank, and (c) the band SPL errors.

methods have almost same octave band patterns in frequency domain. From Table 3, the maximum errors of the filtering and DWT band SPLs are 0.48 and 0.25 dB, respectively, which are all occurred in the octave band with a center frequency of 32 Hz. These errors can make very small contributions to the total SPL values, due to the special frequency characteristics of the vehicle noises. The octave band SPLs from the presented methods are satisfied the error limitation of ± 1 dB published in the IEC 651 standard. The error percentage of the A-weighted total SPLs are 0.2306% and 0.1489% for the filtering and DWT algorithms, respectively. Based on the above comparisons, in conclusion, the presented MF-OBA and DWT-OBA algorithms are effective and feasible for sound quality estimation of vehicle noises, and may be substitutes for the traditional methods used in vehicle SQE engineering.

It should be mentioned the DWT-OBA is a more reasonable and useful method than the MF-OBA. Instead of performing the anti-aliasing low-pass filters and the octave bank filters in the MF-OBA, the DWT-OBA can directly apply a DWT-based filter bank to a target sound signal, which makes it more easily conducted in engineering. The DWT-based filter bank combined by a set of wavelet low- and high-pass filters, has an enough anti-aliasing function for sound OBA. It has been proved in this work that the signal aliasing occurred in the DWT [30] affects the OBA results so little that can be ignored. Due to prominent time-frequency characteristics of the WT, the DWT-OBA can be performed on either the whole length or in slices of a sound

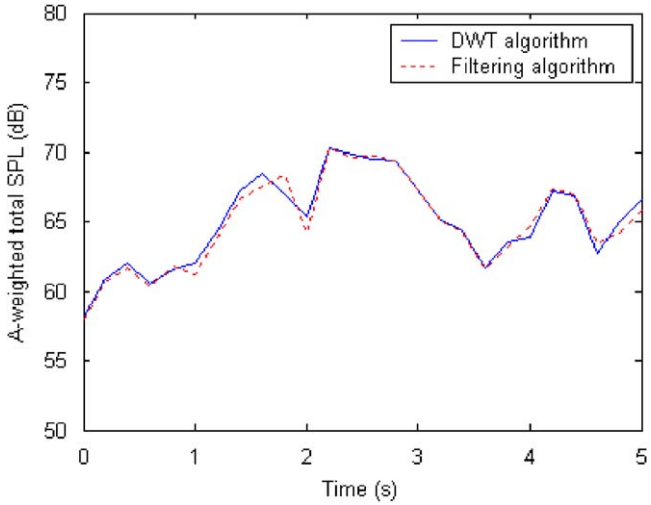

Fig. 16. Calculated time-varying A-weighted total SPLs of the interior vehicle noise by using the newly proposed DWT and filtering algorithms.

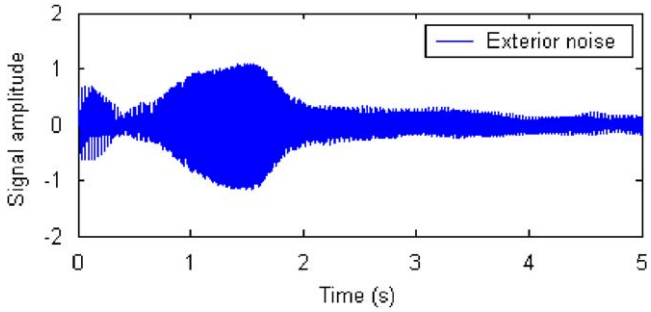

Fig. 17. A measured and denoised exterior noise during vehicle acceleration.

signal and obtain the same results, therefore, is suitable for analyzing nonstationary sound signals. From the OBA results of the interior and exterior vehicle noises, we found that the DWT-OBA is more accurate than the MF-OBA. This may possibly be explained by the anti-aliasing function of the DWT filter bank is more effective than that of the low-pass filters in the MF-OBA algorithm, or by the slight difference in frequency characteristics of the developed two filter banks.

7. Summary and conclusions

This paper presented a new technique for sound quality estimation of vehicle noises. Based on a measured and denoised nonstationary interior noise, firstly, a filter bank including some multirate low-pass and band-pass filters for sound octave analysis was designed, applied and verified by the measured results from a standard sound level meter. According to the frequency characteristics of the filter bank, furthermore, a DWT-based SQE method, the so-called DWT-OBA, was developed and applied to both the interior and exterior vehicle noises. The 35th-order Daubechies wavelet function was determined in establishment of the DWT-OBA filter bank. Verifications show that the DWT-OBA SQE results of the nonstationary vehicle noises are in agreement with the measured ones from the sound level meter, as well as those from the MF-OBA method presented in this work. This implies that the newly developed DWT-OBA and MF-OBA approaches are all effective for SQE of nonstationary vehicle noises; however, in view of the applications, the

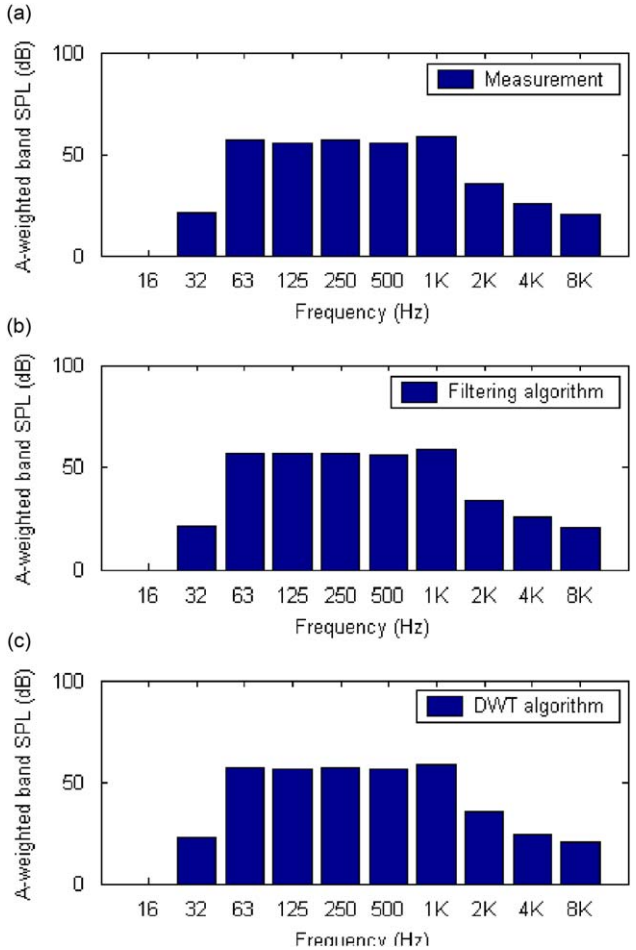

Fig. 18. A-weighted octave-band SPLs of the exterior vehicle noise from (a) the measurement, (b) the self- designed filtering algorithm, and (c) the DWT algorithm.

Table 3
Summary of the calculated A-weighted SPLs of the exterior vehicle noise from different methods.

Octave band number	1	2	3	4	5	6	7	8	9	10
Measured band SPLs (dB)	−13.2	21.0	56.8	55.9	56.7	55.9	58.8	35.4	25.5	20.2
Filtering band SPL errors (dB)	−0.09	0.48	0.05	0.37	0.19	0.12	0	−0.07	0.27	0.17
DWT band SPL errors (dB)	−0.08	0.25	−0.08	0.24	0.09	0.18	0.04	0.02	0.03	−0.01
A-weighted total SPLs (dB)	64.0 (measured), 64.1476 (filtering), 64.0953 (DWT)									
Error percentage of total SPLs	0.2306% (filtering), 0.1489% (DWT)									

Note that the error limitation of octave band SPLs was set to ± 1 dB in the IEC 651 standard.

former is more accurate and feasible than the later. The DWT-OBA can deal with any kind of signal, save computation time, and is a good substitute for the in-situ OBA methods in vehicle SQE engineering.

In applications, the DWT-OBA method can directly be used to estimate and compare sound quality of vehicles, and may be extended not only to other sound signals, such as speech, music, and machinery noise, but also to other engineering fields of signal processing. Applications of the DWT-OBA method to these fields will be promising research topics in the future.

Acknowledgments

This work was supported by the Program for Professor of Special Appointment (Eastern Scholar) at Shanghai Institutions of Higher Learning and the Research Foundation for the Returned Overseas Chinese Scholars of China State Education Ministry, and partly supported by the Research Funds of the Science and Technology Department and the Educational Department of Liaoning Province, China, under Grant nos. 20072198 and 2008RC26.

References

[1] E. Zwicker, H. Fastl, *Psychoacoustics, Facts and Models*, Springer, Berlin, 1990.
[2] H. Fastl, The psychoacoustics of sound-quality evaluation, *Acustica* 83 (1997) 754–764.
[3] F.K. Brandl, W. Biermayer, A new tool for the onboard objective assessment of vehicle interior noise quality, *SAE*, 1999-01-1695, 1999, pp. 1–11.
[4] H. Murata, H. Tanaka, H. Takada, Y. Ohsasa, Sound quality evaluation of passenger vehicle interior noise, *SAE*, 931347, 1993, pp. 675–681.
[5] D. Trapenskas, Sound quality assessment using binaural technology, PhD Thesis, Lulea University of Technology, 2002.
[6] Y.S. Wang, C.-M. Lee, D.-G. Kim, Y. Xu, Sound-quality prediction for nonstationary vehicle interior noise based on wavelet pre-processing neural network model, *Journal of Sound and Vibration* 299 (2007) 933–947.
[7] E. Zwicker, H. Fastl, U. Widmann, K. Kurakata, S. Kuwano, S. Namba, Program for calculating loudness according to DIN 45631 (ISO 532B), *Journal of Acoustic Society of Japan (E)* 12 (1) (1991) 39–42.
[8] E. Zwicker, H. Fastl, C. Dallmayr, BASIC–program for calculating the loudness of sounds from their 1/3-oct band spectra according to ISO 532B, *Acustica* 55 (1984) 63–67.
[9] R. Bisping, Car interior sound quality: experimental analysis by synthesis, *Acustica* 83 (1997) 813–818.
[10] A. Miskiewicz, T. Letowski, Psychoacoustics in the automotive industry, *Acustica* 85 (1999) 645–648.
[11] L. Cohen, *Time-frequency Analysis*, Prentice-Hall, New Jersey, USA, 1995.
[12] B. Gold, N. Morgan, *Speech and Audio Signal Processing*, Wiley, New York, 2000.
[13] B. Hubbard, *The World According to Wavelets: The Story of a Mathematical Technique in the Making*, Wellesley, USA, 1995.
[14] Y.S. Wang, C.M. Lee, L.J. Zhang, Wavelet analysis of vehicle nonstationary vibration under correlation four-wheel random excitation, *International Journal of Automotive Technology* 5 (4) (2004) 257–268.
[15] S.G. Mallat, Z. Zhang, A theory for multiresolution signal decomposition: the wavelet representation, *IEEE Transactions on Pattern Analysis and Machine Intelligence* 11 (1989) 674–691.
[16] N.J. Fliege, *Multirate Digital Signal Processing*, Wiley, New York, 2000.
[17] D.E. Newland, Wavelet analysis of vibration, part I: theory and part II: wavelet maps, *ASME, Journal of Vibration and Acoustics* 116 (1994) 409–425.
[18] L.H. Yam, Y.J. Yan, J.S. Jiang, Vibration-based damage detection for composite structures using wavelet transform and neural network identification, *Composite Structure* 60 (2003) 403–412.
[19] P.D. Samuel, D.J. Pines, Constrained adaptive lifting and the CAL4 metric for helicopter transmission diagnostics, *Journal of Sound and Vibration* 319 (2009) 698–718.
[20] N. Roy, R. Ganguli, Helicopter rotor blade frequency evolution with damage growth and signal processing, *Journal of Sound and Vibration* 283 (2005) 821–851.
[21] B.F. Yan, A. Miyamoto, E. Brühwiler, Wavelet transform-based modal parameter identification considering uncertainty, *Journal of Sound and Vibration* 291 (2006) 285–301.
[22] N. Roy, R. Ganguli, Filter design using radial basis function neural network and genetic algorithm for improved operational health monitoring, *Applied Soft Computing* 6 (5) (2006) 154–169.
[23] GB 1495-2002: Limits and Measurement Methods for Noise Emitted by Accelerating Motor Vehicles, 2002.
[24] R. Verma, R. Ganguli, Denoising jet engine gas path measurements using nonlinear filters, *IEEE/ASME Transactions on Mechatronics* 10 (4) (2005) 461–464.
[25] V.P. Surender, R. Ganguli, Adaptive myriad filter for improved gas turbine condition monitoring using transient data, *Journal of Engineering for Gas Turbine and Power* 127 (2) (2005) 329–339.
[26] R. Ganguli, Noise and outlier removal from jet engine health monitoring signals using weighted FIR median hybrid filters, *Mechanical Systems and Signal Processing* 16 (6) (2002) 967–978.
[27] IEC-1260: Electroacoustics: Octave-Band and Fractional-Octave-Band Filters, 1995.
[28] I. Daubechies, The wavelet transform, time frequency localization signal analysis, *IEEE Transactions on Information Theory* 36 (1990) 961–1005.
[29] E. Zwicher, Procedure for calculating loudness of temporally variable sounds, *Journal of the Acoustical Society of America* 62 (1977) 675–682.
[30] J. Yang, S.-T. Park, An anti-aliasing algorithm for discrete wavelet transform, *Mechanical System and Signal Processing* 17 (5) (2003) 945–954.